Tuning 3C-SiC(100)/ Si(100) heterostructure interface quality

Maddalena Pedio[1], Elena Magnano[1,2], Paolo Moras [3], Francesco Borgatti[4], Roberto Felici[5], Barbara Troian [6], Stefano Prato[6], Cristian Soncini[1,7], and Cinzia Cepek[1]*

[1]Istituto Officina dei Materiali, Consiglio Nazionale delle Ricerche, Area Science Park, Strada Statale 14 km 163.5, I-34149 Trieste, Italy

[2] Department of Physics, University of Johannesburg, PO Box 524, Auckland Park, 2006 Johannesburg, South Africa

[3] Istituto di Struttura della Materia, Consiglio Nazionale delle Ricerche, Strada Statale 14 km 163.5, I-34149 Trieste, Italy

[4]Consiglio Nazionale delle Ricerche-Istituto per lo Studio dei Sistemi Nanostrutturati (CNR-ISMN), Sezione di Bologna, Italy

[5] SPIN-CNR, Area della Ricerca di Tor Vergata, Via del Fosso del Cavaliere 100, 00133 Roma, Italy

[6] A.P.E. Research S.r.l., Area Science Park, Basovizza I-34149 Trieste, Italy

[7] Department of Physics, University of Trieste, I-34127 Trieste, Italy

* soncini@iom.cnr.it

KEYWORDS Silicon Carbide, 3C-SiC, Heterostructure, Interfacial defects, Surface, Thin films, SNOM, Photoemission, Inverse Photoemission.

ABSTRACT We report on a systematic spectroscopic and structural investigation of 3C-silicon carbide (3C-SiC) films grown on Si(100)-(2×1) by co-deposition of C_{60} molecules and Si atoms in ultra-high vacuum conditions. This work focuses on reducing the macroscopic defects formed at the interface in Si-SiC heterojunctions. A wide range of parameters influences the growth process, including the substrate deposition temperature, the relative effusion fluxes of C_{60} and Si, and the clean Si(100) surface order. By adjusting the Si and C_{60} deposition rates, it is possible to reduce the Si atom diffusion from the substrate and control both the surface morphology and the specific formation of the C-rich c(2×2) or the Si-rich 3×2 ordered surfaces. Our results show that the growth of 3C-SiC on flat and good quality Si substrates is a crucial and necessary starting point to obtaining good quality 3C-SiC/Si interfaces with a minimum number of defects.

Introduction

The current emerging tendency toward sustainable green technology requires the development of new high-performance microelectronic devices with an increased power density and reduced cooling requirements. In this framework, the remarkable mechanical and electrical properties of the silicon carbide (SiC)[1-4] make it a material of great interest in the power device industry as an alternative route to Si-based devices in sustainable modern technology. Its physical properties allow operation for many applications, including harsh environments and high temperatures, as well as the optimization of the electronic device through faster switching speed, lower losses and higher blocking voltages with respect to Si-based technology. To date, most of the fundamental research related to the SiC is focused on hexagonal polymorphs 4H and 6H, and high-grade single-crystal wafers are commercially available. However, in the last years, the cubic polytype (3C-SiC) has been attracting notable interest in the scientific community thanks to its remarkable technological benefits to hexagonal polymorphs[5]. Due to the lower bandgap of 3C-SiC (2.35 eV) compared to 4H- and 6H-SiC (3.28 eV and 3.08 eV respectively), a lower density of interface

states is expected at the 3C-SiC/SiO_2 interface. As a consequence, field-effect transistors based on 3C-SiC have the highest channel mobility ever observed in any SiC polytype, implying a remarkable reduction in power consumption. Furthermore, the much lower temperature coefficient of resistance between the operating temperature of the device and the room temperature (RT) of 3C-SiC leads to a drastic reduction of the device-on-resistance. Last but not least, the 3C-SiC polytype is the only one that can be grown on cheap Si substrates[6,7]. It is obtained at the lowest growth temperature among the SiC polymorphs, offering a real economic benefit in the growing cost, the potential for faster scale-up with substrate wafer size and the direct integration into the presently available Si technology. For those reasons, the growth of high-quality 3C-SiC epilayers and bulk wafers is becoming a key aspect for its integration into commercial power devices. Nevertheless, despite the large efforts in the last years, the fabrication of low-cost and high-quality 3C-SiC on Si is still a crucial issue[8].

Though the 3C-SiC heteroepitaxial growth on 4H- and 6H-SiC has been optimized[9,10,11], the growth on Si substrates presents important limiting factors to obtain device-grade growth of 3C-SiC/Si heterojunctions; the large crystallographic mismatch between the bulk lattice parameters of Si and 3C-SiC (~19%), and the difference between the thermal expansion coefficients of the two materials (~8% at RT and ~23% at the typical growth temperature). These facts lead to a high density of structural defects, hampering the synthesis of device-quality 3C-SiC/Si heterostructures[6,7,8,12]. Furthermore, the significant Si diffusion from the substrate, which occurs at typical growth temperatures, implies the formation of pyramidal pits, “vulcan-like” structures and voids at the interface between the substrate and the growing films[12-15]. Many strategies have been used to overcome these problems, such as substrate pre-patterning[16-19], opportune gasses mixtures[12,20 and refs therein, 21] and the use of a buffer layer[22-25]. Nevertheless, the problem is far from being solved. SiC growth by chemical vapour deposition (CVD) is normally performed using precursors mixtures of silane, hydrocarbons and various Si/organic compounds in a hydrogen

flow. In literature, the dimension of the voids at the interface can be modulated by the C/H ratio, the carbonization time and the H etching time (during the temperature ramp-up between carbonization and growth). Last but not least, the presence of undesired residuals of SiO_x at the 3C-SiC/Si interface can affect the transport properties at the interface in an uncontrolled way, dramatically decreasing the device performance[26-29].

Among all the many growth methods and precursors exploited so far, the C_{60} molecules have been successfully used as a carbon source to synthesize 3C-SiC films on Si substrates, even if the interface shows several defects[30-37]. As we demonstrate in the following, the appropriate choice of co-deposited Si and C_{60} fluxes and growth temperature allows the reduction of the Si atoms effusion from the substrate, which is the main responsible for the large number of defects and voids formation at the interface. Moreover, by using Si and C_{60}, no extra chemical species are present in the precursors limiting the chemical contamination of the grown SiC layer (H-free). On the other hand, the preparation of the Si substrate and the deposition conditions influence the microstructure within the SiC film. The quality of the substrate (in terms of contaminants and defects) is crucial to obtain, both morphologically and structurally, good quality SiC films and interfaces. Indeed, the morphology of the thin films reflects the morphology of the substrate, such as the number of defects of the grown film is related to the number of defects of the substrate surface itself [38]. Generally, samples obtained by co-deposition (showing pits of pyramidal shape at the SiC/Si interface and holes on the surface[20,30-37,39-42]) are grown by using high growth flux rate and poor base pressures ($\approx 1\times10^{-7}$ mbar-1×10^{-8} mbar), conditions in which it is extremely hard to obtain well-ordered, flat, and defect-free clean Si substrates[43,44].

This work reports a systematic spectroscopic and structural-morphologic investigation of 3C-SiC films grown on Si(100)-(2×1) by co-deposition of C_{60} precursor molecules and Si atoms. Particular attention is devoted to minimizing the macroscopic defects formed at the interface in Si-SiC heterojunctions. All the samples were prepared in ultra-high vacuum conditions (UHV),

at a base pressure of ~5×10^{-11} mbar. We spanned over a wide range of parameters that influence the growth process, including the substrate deposition temperature, the relative effusion fluxes of C_{60} and Si, and the surface order of the clean Si(100) surface. The growth in UHV conditions avoids the formation of SiO_x at the interface and the presence of contaminants, resulting in an increased quality of the heterostructure and improved reproducibility of its electronic properties. The UHV growth also results in good surface quality of the 3C-SiC layers. The growth and the experimental approach used enabled us to check *in-situ* through a variety of surface-science experimental techniques, the quality, stoichiometry and purity of the starting substrates and the grown films, avoiding any possible artefact induced by contaminants. The *in-situ* available experimental techniques were low energy electron diffraction (LEED), ultra-violet and X-ray photoemission spectroscopy (UPS and XPS, respectively), and inverse photoemission spectroscopy (IPS).

Taking advantage of the transparency of SiC to visible light, we studied the 3C-SiC/Si(100) interface of our films *ex-situ* by using conventional optical microscopes and scanning near field optical microscope (SNOM) with a spatial resolution of 50-100 nm. The crystallinity of the most promising samples was determined by *ex-situ* X-ray diffraction (XRD) and X-ray reflectivity (XRR). From XRD analysis we obtained information on the long-range order structure of the grown film, i.e. the domain size along with the main crystallographic directions, while by XRR we have determined the film thickness, its density, and the surface as well as the 3C-SiC/Si interface roughness.

Experimental section

All synthesis were performed by using un-doped Si(100) Siltronix wafers. The C_{60} and Si co-deposition was performed in UHV conditions on clean, well-ordered reconstructed Si(100)-2×1 surfaces and on not-reconstructed Si(100) surfaces. The ordered Si(100)-2×1 surfaces were

obtained by annealing the substrate up to 1200-1300 K maintaining the pressure below 1×10^{-9} mbar during the whole process. In these conditions, the produced surfaces are flat, well ordered and with a low number of defects [43,44]. The so-obtained surfaces show sharp double domains 2×1 LEED patterns, and sharp surface states in the valence (VB) and conduction band (CB) spectra (see Figure 1), in agreement with previous measurements [45]. The non-reconstructed surfaces (1×1 LEED pattern) were obtained by flashing the Si(100) substrate in poor vacuum conditions (>9×10^{-9}mbar). Annealing in these conditions leads to the presence of a large number of defects [43,44]. No contaminants (in particular oxygen and/or carbon) were observed in the photoemission spectra in both cases.

Pure C_{60} (99.9%), purchased from Sigma Aldrich, was sublimated from a tantalum crucible, while Si deposition was obtained by resistive heating of a p-doped Si wafer. The C and Si fluxes and coverages were measured employing XPS. The fluxes were determined by depositing C_{60} on Si(100), and Si on a poly-crystalline copper plate at ≈300 K, assuming a unitary sticking coefficient for both at this temperature. During C_{60} and Si co-sublimation the pressure in the preparation chamber was always lower than $4.0\text{x}10^{-9}$ mbar. The UPS spectra were obtained by using a conventional He discharge lamp ($h\upsilon$= 21.2 eV and 40.8 eV), while the XPS spectra by means of a conventional Mg K_α X-ray source ($h\upsilon$= 1253.6 eV). The electron energy distribution curves were measured in normal emission geometry with a 100 mm-radius hemispherical electron energy analyser (acceptance angle ≈7°). The overall instrumental energy resolution was 120 meV for the UPS VB spectra and 1.2 eV for the XPS core level spectra. All the binding energies of the VB and core level spectra have been referenced, respectively, to the Fermi (E_F) and Ag 3*d* core levels of a silver target in direct contact with the sample.

The normal incidence IPS measurements were performed in UHV using a homemade Erdman-Zipf electron gun. The electron beam divergence was better than 3°. Photons emitted from the sample surface were collected by a homemade Geiger-Müller type detector with a He-I_2 gas

mixture and an SrF_2 entrance window filtering photons of 9.5 eV. The experimental resolution was better than 300 meV, as measured by the E_F onset of a clean Ta foil. The spectra were normalized at each point to the incident electron beam current.

SNOM topography and near-field measurements were performed by using a TriA-SNOM microscope (A.P.E. Research, Trieste, Italy) in illumination mode. In this setup, the light coming from a laser source is coupled with a single-mode optical fiber. The scattered light from the sample surface can be collected both in reflection and transmission mode. The TriA-SNOM microscope is provided with a flexure scanning stage with a maximum in-plane XY scan area of 100 μm x 100 μm and z-scan range of 10 μm, equipped with strain gauge sensors to provide an absolute positioning. In this work, SNOM topography and optical reflection measurements were simultaneously performed by using a laser source with 650 nm wavelength, and a pulled SNOM fiber probe of 50 nm nominal tip aperture (Lovalite, Besancon, France).

The crystallinity of the SiC films has been characterized by XRD using a commercial PanalyticalX'pert with a Cu X-ray source. Surface XRD and XRR measurements of the 3×2 SiC sample were performed at the ID03 beamline at ESRF (Grenoble)[46]. All measurements were performed at RT.

Results and Discussion

The substrate temperature during the sample growth is a key parameter to obtain high-quality 3C-SiC films and interfaces requiring to be carefully controlled. As mentioned above, the high density of structural defects at the interface strongly depends on the different thermal expansion coefficients of Si and 3C-SiC[7], and the diffusion of Si atoms through defects of the substrate surface (as discussed for example in refs[7,30,36,47]). As a consequence, the growth temperature must be chosen as low as possible, but at the same time, it must be high enough to allow the formation of 3C-SiC layers with high crystallographic properties. Three different growth

temperatures were selected, 1050 K (minimum temperature to form SiC[33,36]), 1200 K and 1370 K, corresponding to three significantly different growth conditions. At 1050 K the reaction time (time necessary for the complete reaction of C_{60} molecules with the Si substrate to form covalent Si-C bonds obtaining SiC, as shown in ref. 33 and references therein) is rather slow, about 300 s[43], and the possibility to grow well-ordered samples might be reached only by fixing the C_{60} flux to a low rate, as discussed below. At 1200 K the reaction time is remarkably shorter, about 5 s, while at 1370 K the reaction time is <1s[33-37]. The C_{60} deposition rate was fixed at 0.1 monolayers (ML) per minute (i.e. $1.15\times10^{13}\pm$ 5% carbon atoms cm^{-2} s^{-1}) for all samples, which corresponds to the complete reaction of the C_{60} molecules at the lowest growing temperature (1050 K). A detailed description of the C_{60} monolayer calibration and definition can be found in Ref. 34. The Si atoms flux was fixed to 70% and 100% of the C flux. The films had a thickness in the range of 0.1-0.5 μm.

Sample name	Growth T (K) and C_{60} reaction time	Silicon substrate LEED	Si:C co-deposition flux	3C-SiC LEED	C% (via XPS)
S1_1050_70	1050 (300s)	1x1	70:100	NO	50
S1_1050_100			100:100	NO	50
S2_1050_70		2x1	70:100	NO	50
S2_1050_100			100:100	NO	50
S1_1200_70	1200 (5s)	1x1	70:100	NO	50
S1_1200_100			100:100	NO	50
S2_1200_70		2x1	70:100	c(2x2)	48
S2_1200_100			100:100	3x2	50
S1_1370_70	1370 (<1s)	1x1	70:100	NO	50
S1_1370_100			100:100	NO	50
S2_1370_70		2x1	70:100	3x2	46
S2_1370_100			100:100	3x2	46

Table 1. Summary of the growth parameters and the surface reconstructions of the studied 3C-SiC films**.** The sample names are defined as Sx_temp_flux, where Sx is the silicon

substrate surface reconstruction 1×1 (S1) or 2×1 (S2), temp is the growth temperature, and flux is the Si:C flux ratio used during deposition. The sample stoichiometry and C % have been determined by XPS (Supporting Information).

Table1 summarizes our results. Independently of the substrate quality and Si fluxes, the 3C-SiC samples grown at the lowest temperature (1050 K) are stoichiometric, as confirmed by XPS (Supporting Information). However, their surfaces are not ordered: they do not show any LEED pattern nor surface states in the VB and CB. As an example, the sample S2_1050_70 shown in Figure 1.

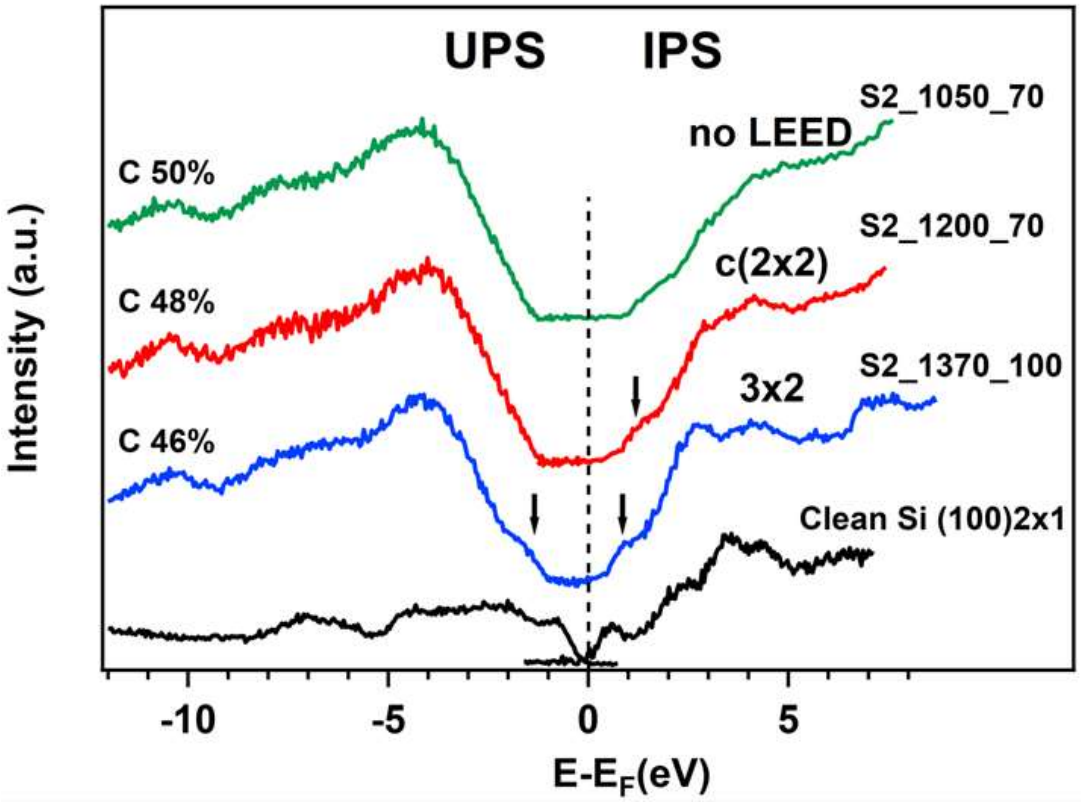

Figure 1. Combined UPS-IPS spectra of samples S2_1050_70, S2_1200_70 and S2_1370_100 compared to the clean 2×1 reconstructed Si(100) surface. The arrows indicate the features interpreted as filled and empty surface states. See text for more details.

The electronic properties of the 3C-SiC films were characterized by combined UPS-IPS measurements. The spectra are shown in Figure 1 together with the Si(100) 2×1 spectrum for comparison[45]. Samples with (3×2) or c(2×2) LEED patterns show a weak shoulder at about -0.8 eV in the UPS spectra, the distinctive feature of a surface state[48-50]. Our results are in good agreement with the literature VB measurements, though the energy and angular resolutions in this work do not allow us to better resolve it. On the other hand, thanks to the IPS angular resolution the CB spectra show a defined structure at about 1.1 eV assigned to C-Si empty states[51-53], even in the polycrystalline SiC films[32]. The broad feature at higher energies of the polycrystalline sample (S2_1050_70) becomes sharper and structured as the long-range surface order increases. In particular, the (3x2) reconstructed 3C-SiC(100) shows two unoccupied surface states at 0.6 eV and 2.3 eV, while in the c(2×2) the surface states are located at about 2.9 eV and 5 eV. The IPS spectra of the two ordered phases, 3×2 and c(2×2) SiC(100) [52-54], are in good agreement with the literature, confirming the electronic structure of Si-rich 3×2 SiC(100) and C-rich c(2×2) SiC(100).

Independently of the growth temperature, no LEED pattern and a large number of interface defects were observed in all samples grown on non-reconstructed surfaces (1×1), pointing out the importance of the substrate quality. In these cases, the optical microscope images show a large number of rectangular structures with average sizes in the μm scale. An example is reported in Figure 2a (sample S1_1050_70). These results are in agreement with the typical pyramidal shape pits of the SiC/Si(100) interface already reported in the literature[7,30,36,39,47]. The observed defects have an interface area density of about 50% displaying the same organization as the typical defects of Si(100) surfaces annealed in bad vacuum conditions. We expect their presence already before the co-deposition procedure, as reported in the literature[47,55].

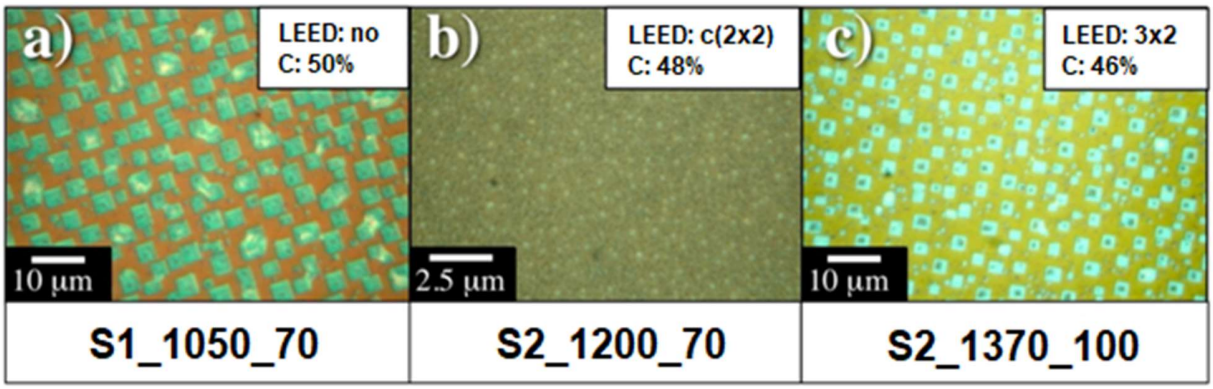

Figure 2. Optical microscope images, showing the pits at the 3C-SiC/Si(100) interface of samples **a)** S1_1050_70 (interface defects area 50.4%), **b)** S2_1200_70 (interface defects area 3.8%) and **c)** S2_1370 (interface defects area 39%). The interface defects area has been estimated by means of the software for image analysis *gwyddion*[56].

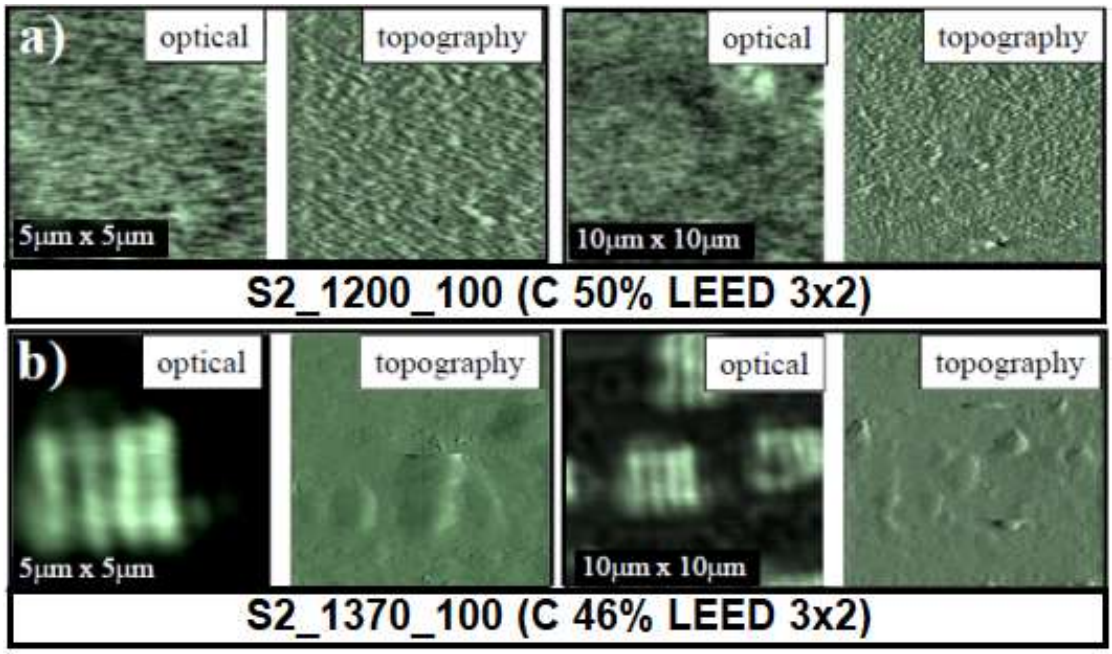

Figure 3. Ex-situ SNOM optical of samples **a)** S2_1200_100 and **b)** S2_1370_100. SNOM reflection (left) at a wavelength of 650 nm, and simultaneous SNOM topography (right) on different scan areas (5mµ × 5mµ and 10mµ × 10mµ). The interference fringes in the

SNOM optical images of the sample S2_1370_100 are due to light reflection inside the interface pits/holes.

Concerning the samples S2_1200_70 and S2_1200_100, grown at 1200 K, both show a long-range order at the 3C-SiC surface, as confirmed by LEED (Table 1) and by the presence of surface electronic states in the combined UPS-IPS spectra (Figure 1). The topmost layers of the films have different LEED patterns and surface electronic states, typical of 3C-SiC(100) terminated surfaces: the c(2×2) pattern corresponds to a C-terminated surface, while the 3×2 to a Si-terminated surface[48]. The surface reconstruction was found to be dependent on the Si/C flux ratio. By using a 70% Si/C flux ratio, the samples show a c(2×2) LEED pattern, while fixing the Si/C flux ratio at 100% the 3×2 surface reconstruction is observed. By changing the relative Si/C fluxes it is possible to modulate the surface morphology, obtaining different surface reconstructions in controlled conditions. As shown in Figure 2b, the sample S2_1200_70 (c(2×2) LEED pattern; C concentration: 48%) has the lower density and dimension of defects at the 3C-SiC/Si(100) interface (interface defects area 3.8%). In the S2_1200_100 sample (3×2 LEED pattern; C concentration 50%) almost no defects are visible at the optical microscope. This is also confirmed by SNOM measurement at higher lateral resolution (Figure 3a). The typical mean roughness as measured by SNOM was <2 nm. We recall that SNOM allows acquiring the optical and the topography images of the same area of the sample, at the same time. The negligible number of holes in the topography and in the optical image indicates that if pits are present at the interface, their lateral dimensions are smaller than the SNOM optical resolution, i.e. ≈ 80 nm. This result suggests that the Si flux used in this case was enough to deplete the diffusion of the Si atoms from the substrate, resulting in a strong decrease in defect formation at the interface. The samples S2_1370_70 and S2_1370_100, grown at 1370 K, have the same 3×2 LEED patterns (Si terminated surface) and stoichiometry (C concentration 46%). This may be due to a significantly

different sticking coefficient of the C_{60} at 1370 K with respect to 300 K. At 1370 K, a considerable fraction of C atoms may desorb from the surface before reacting. Moreover, at this temperature, the Si diffusion from the substrate is higher, and the 3C-SiC films show again a considerable number of defects at the interface (Figures 2c and 3b).

The crystallinity and orientation of the 3C-SiC films S2_1370_70 and S2_1370_100 were confirmed by *ex-situ* XRD using a standard laboratory diffractometer with a Cu K-alpha radiation source. The θ-2θ patterns (not shown) exhibit the characteristic peaks at θ= 41.7° at θ= 69.8° assigned in the literature (see for example ref. 57) to the (002) 3C-SiC and (004) Si reflections, respectively. Figure 4 shows the rocking curve around the [-1 0 1] 3C-SiC Bragg peak measured at the ID03 of the ESRF facility[46]. The in-plane FWHM of the peak is better than 0.017 r.l.u. (relative lattice unit), which in SiC films, corresponds to a lateral domain size ≥ 25 nm [58].

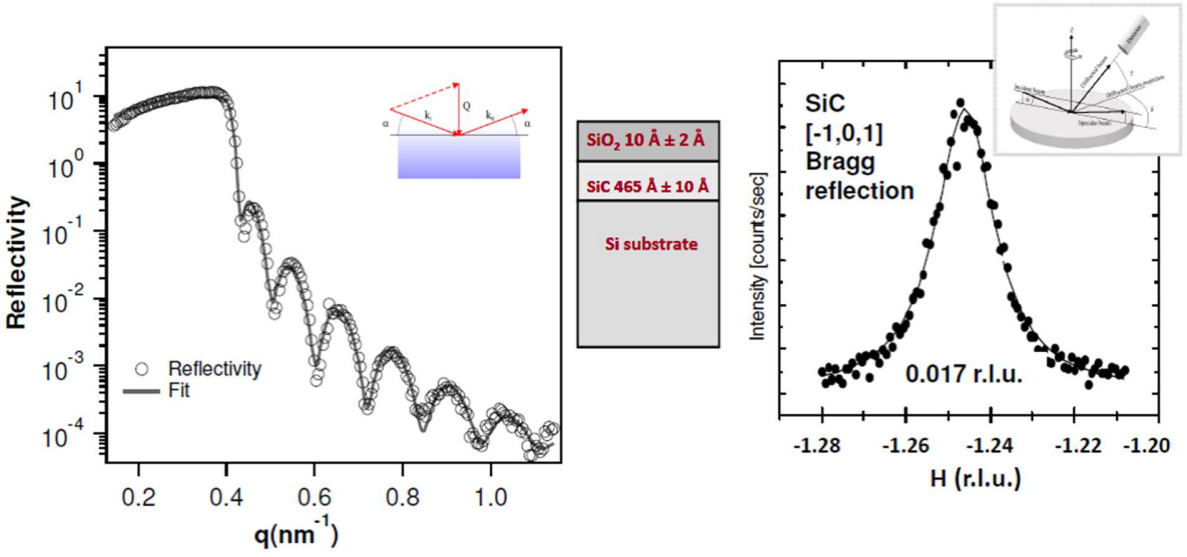

Figure 4. X-ray reflectivity *(left)* and rocking curve around the [-1 0 1] Bragg peak *(right)* of the S2_1370_70 sample. The analysis is described in the text.

By XRR measurements we were able to determine the density of the 3C-SiC film along with its electronic density, surface roughness and inter-diffusion layer. The XRR data and its fit of the sample S2_1370_70 are shown in Figure 4. The data were fitted using the GenX software[59] and a sample model made of the Si substrate, a SiC film of 46.5 ±0.3 nm and a native SiO_2 top layer of a few Å[60]. According to the best fit (continuous line), the electronic density of the SiC layer is 1.00±0.02 e $Å^{-3}$, in very good agreement with the theoretical value (0.97 e $Å^{-3}$) of the 3C-SiC. To fit the data correctly, it was necessary to simulate the presence of the pits on the Si substrate. This was achieved by introducing in the model, between the SiC and the Si substrate, a fictitious layer having an electronic density about half the value of the SiC layer and thickness of about 10 nm. We should stress that the XRR data are very sensitive to the thickness and density of the SiC layer, as well as to the presence of a layer between the SiC and the substrate having a density smaller than the ones of the SiC and Si. On the other hand, the data are quite insensitive to the thickness and inter-diffusion values of the fictitious layer.

Conclusions

In summary, we found that the quality of the 3C-SiC/Si(100) interface strongly depends on the clean Si(100) substrate quality, the C and Si atoms fluxes, and the substrate growing temperature. The best 3C-SiC quality was obtained on well-clean and reconstructed Si(100)-2×1 surfaces. Depending on the Si and C_{60} deposition rates it is possible to control the 3C-SiC surface morphology and the formation of the C-rich, c(2×2), or of the Si-rich, 3×2, ordered surfaces. The lower number of defects at the SiC/Si interface was obtained at 1200 K and Si:C flux fixed at 70%. This study provides useful insights to optimize the growth and control the physical properties of 3C-SiC/Si heterojunctions. A detailed understanding of the main factors influencing the quality of the 3C-SiC/Si(100) interface is crucial for future technological applications of this material in commercial power devices, and its integration into the currently

available Si-based technology. Further analysis is planned to characterize the defects within the SiC film, i.e. stacking faults and anti-phase boundary at the micro and nanoscale, fundamental for electronic applications of 3C-SiC.

Supporting Information

XPS characterization of the samples S2_1200_70 and S2_1050_70 (PDF)

AUTHOR INFORMATION

Corresponding Author

soncini@iom.cnr.it

Author Contributions

C. Cepek and M. Pedio conceived and planned the experiment, C. Cepek, M. Pedio, E. Magnano, P. Moras and C. Soncini contributed to the growth of the samples and carried out the spectroscopic characterization (XPS, UPS and IPS measurements), E. Magnano, B. Troian and S. Prato performed the optical microscope images and the SNOM measurements, R. Felici and F. Borgatti carried out the XRR measurements and performed the simulation of the XRR data. All authors discussed the results and approved the final version of the manuscript.

Funding Sources

Project partially supported by the Italian MIUR through the Progetto Eurofel.

Acknowledgement

The CNR-IOM technical staff, Federico Salvador, Paolo Bertoch, Davide Benedetti, Stefano Bigaran and Andrea Martin, is kindly acknowledged for their support. Beamtime at ESRF, (Grenoble, France) was provided at the ID03 beamline under proposal SI-819.

References

(1) She, X.; Huang, A. Q.; Lucia, O.; Ozpineci, B. Review of Silicon Carbide Power Devices and Their Applications. IEEE Transactions on Industrial Electronics 2017, 64, 8193-8205.

(2) Casady, J.B.; Johnson, R.W. Status of silicon carbide (SiC) as a wide-bandgap semiconductor for high-temperature applications: A review. Solid-State Electronics 1996, 39, 1409-1422.

(3) Maboudian, R.; Carlo Carraro, C.; Senesky, D. G.; Roper, C.S. Advances in silicon carbide science and technology at the micro- and nanoscales. Journal of Vacuum Science & Technology A 2013, 31, 050805.

(4) Kimoto T.; Cooper J.A.; Fundamentals of Silicon Carbide Technology. IEEE, Wiley, 2014.

(5) La Via, F.; Zimbone, M.; Bongiorno, C.; La Magna, A.; Fisicaro, G.; Deretzis, I.; Scuderi, V.; Calabretta, C.; Giannazzo, F.; Zielinski, M.; Anzalone, R.; Mauceri, M.; Crippa, D.; Scalise, E.; Marzegalli, A.; Sarikov, A.; Miglio, L.; Jokubavicius, V.; Syväjärvi M.; Yakimova, R.; Schuh, P.; Schöler, M.; Kollmuss, M.; Peter, P. New Approaches and Understandings in the Growth of Cubic Silicon Carbide. Materials 2021, 14, 5348.

(6) Ferro, G. 3C-SiC Heteroepitaxial Growth on Silicon: The Quest for Holy Grail. Critical Reviews in Solid State and Materials Sciences 2015, 40, 56–76.

(7) Li, Y.; Zhao, Z; Yua, L.; Wang, Y; Yin, Z.; Li, Z.; Han, P. Heteroepitaxial 3C-SiC on Si (100) with flow-modulated carbonization process conditions. Journal of Crystal Growth 2019, 506, 114–116.

(8) Chaussende, D.; Mercier, F.; Boulle, A.; Conchon, F.; Soueidan, M.; Ferro, G.; Mantzari, A.; Andreadou, A.; Polychroniadis, E.K.; Balloud, C.; Juillaguet, S.; Camassel, J.; Pons, M. Prospects for 3C-SiC bulk crystal growth. J. Cryst. Growth 2008, 310, 976-981.

(9) Soueidan, M.; Ferro, G. A Vapor–Liquid–Solid Mechanism for Growing 3C-SiC Single-Domain Layers on 6H-SiC(0001). Adv. Funct. Mater. 2006, 16, 975-979.

(10) Powell, J.A.; Larkin, D.J.; Matus, L.G.; Choyke, W.J.; Bradshaw, J.L.; Henderson, L.; Yoganathan, M.; Yang, J.; Pirouz, P. Growth of improved quality 3C-SiC films on 6H-SiC substrates. Appl. Phys. Lett. 1990, 56, 1353-1355.

(11) La Via F.; Severino A.; Anzalone R.; Bongiorno, C.; Litrico G.; Mauceri M.; Schoeler M.; Schuh P.; Wellmann P. From thin film to bulk 3C-SiC growth: Understanding the mechanism of defects reduction. Materials Science in Semiconductor Processing 2018, 78, 57-68.

(12) Gupta, A.; Sengupta, J.; Jacob, C. An atomic force microscopy and optical microscopy study of various shaped void formation and reduction in 3C-SiC films grown on Si using chemical vapor deposition. Thin Solid Films 2008, 516, 1669–1676.

(13) Kim, K. C.; Park, C. I.; Roh, J. I., Nahm, K. S.; Seo, Y. H. Formation mechanism of interfacial voids in the growth of SiC films on Si substrates. J. Vac. Sci. Technol. A 2001, 19, 2636-2641.

(14) Anzalone, R.; Litrico, G.; Piluso, N.; Reitano, R.; Alberti, A.; Fiorenza, P.; Coffa, S.; La Via, F. Carbonization and transition layer effects on 3C-SiC film residual stress. J. Cryst. Growth 473 (2017) 11–19.

(15) Nagasawa, H.; Yagi, K.; Kawahara, T.; Hatta, N. Reducing Planar Defects in 3C–SiC. Chem. Vap. Depos. 2006, 12, 502–508.

(16) Nagasawa, H.; Kawahara, T.; Yagi, K.; Hatta, N.; Uchida, H.; Kobayashi, M.; Reshanov, S.; Esteve, R.; Schöner, A. High Quality 3C-SiC Substrate for MOSFET Fabrication. Mater. Sci. Forum 2012, 711, 91–98.

(17) La Via, F.; D'Arrigo, G.; Severino, A.; Piluso, N.; Mauceri, M.; Locke, C.; Saddow, S.E. Patterned substrate with inverted silicon pyramids for 3C–SiC epitaxial growth: A comparison with conventional (001) Si substrate. J. Mater. Res. 2013, 28, 94-103.

(18) von Känel, H.; Isa, F.; Falub, C.V.; Barthazy, E.J.; Müller, E.; Chrastina, D.; Isella, G.; Kreiliger, T.; Taboada, A.G.; Meduňa, M.; Kaufmann, R.; Neels, A.; Dommann, A.; Niedermann, P.; Mancarella, F.; Mauceri, M.; Puglisi, M.; Crippa, D.; La Via, F.; Anzalone, R.; Piluso, N.; Bergamaschini, R.; Marzegallik, A.; Miglio, L. Three-Dimensional Epitaxial $Si_{1-X}Ge_x$, Ge and SiC Crystals on Deeply Patterned Si Substrates ECS Trans. 2014, 64, 631–648.

(19) Md Foisal, A. R.; Nguyen, T.; Dinh, T.; Nguyen T. K.; Tanner, P.; Streed, E. W.; Dao, D. V. 3C-SiC/Si Heterostructure: An Excellent Platform for Position-Sensitive

Detectors Based on Photovoltaic Effect. ACS Appl. Mater. Interfaces 2019, 11, 40980−40987.

(20) Zimbone, M.; Mauceri, M.; Litrico, G.; Barbagiovanni, E.; Bongiorno, C.; La Via, F. Protrusions reduction in 3C-SiC thin film on Si. Journal of Crystal Growth 498 (2018) 248–257.

(21) Nishino, S.; Powell, J.; Will, H.A.; Production of large-area single-crystalwafers of cubic SiC for semiconductor devices. Appl. Phys. Lett. 1983, 42, 460-462.

(22) Masri, P.; Moreaud, N.; Rouhani Laridjani, M.; Calas, J.; Averous, M.; Chaix, G.; Dollet, A.; Berjoan, R.; Dupuy, C. The physics of heteroepitaxy of 3C–SiC on Si: role of Ge in the optimization of the 3C–SiC/Si heterointerface. Mater. Sci. Eng. B 1999, 61–62, 535–538.

(23) Sarney, W.L.; Wood, M.C.; Salamanca-Riba, L.; Zhou, P.; Spencer, M. Role of Ge on film quality of SiC grown on Si J. Appl. Phys. 2002, 91, 668-671.

(24) Piluso, N.; Camarda, M.; Anzalone, R.; Severino, A.; Scalese, S.; La Via, F. Analysis on 3C-SiC Layer Grown on Pseudomorphic-Si/Si1-xGex/Si(001) Heterostructures. Mater. Sci. Forum 2014, 806, 21–25.

(25) Chaudhry, M.I. Electrical properties of β-SiC metal-oxide-semiconductor structures. J. Appl. Phys. 1991, 69, 7319- 7321.

(26) Afanasev, V.V.; Bassler, M.; Pensl, G.; Schulz, M. Intrinsic SiC/SiO_2 Interface States. Phys. Status Solidi (a) 1997, 162, 321-337 and references therein.

(27) Schoner, A.; Krieger, M.; Pensl, G.; Abe, M.; Nagasawa, H. Fabrication and Characterization of 3C-SiC-Based MOSFETs. Chem. Vap. Depos. 2006, 12, 523-530.

(28) Takahashi, M.; Im, S.-S.; Madani, M.; Kobayashi, H. Nitric Acid Oxidation of 3C-SiC to Fabricate MOS Diodes with a Low Leakage Current Density Semiconductor Devices, Materials, and Processing J. Electrochem. Soc. 2008, 155, H47-H51.

(29) Constant, A.; Camara, N.; Placidi, M.; Decams, J.-M.; Camassel, J.; Godignon, P. Interfacial Properties of Oxides Grown on 3C-SiC by Rapid Thermal Processing Dielectric Science and Materials J. Electrochem. Soc. 2011, 158, G13-G19.

(30) Volz, K. K.; Schreiber, S.; Gerlach, J.W.; Reiber, W.; Rauschenbach, B.; Stritzker, B.; Assmann W.; Ensinger, W. Heteroepitaxial growth of 3C-SiC on (100) silicon by C_{60} and Si molecular beam epitaxy. Mat. Sci. & Engineering 2000, 289, 255.

(31) Moras, P.; Mahne, N.; Ferrari, L.; Pesci, A.; Capozi, M.; Aversa, L.; Jha, S.N.; Verucchi,. R.; Iannotta, S.; Pedio M., SiC ordered film growth by C_{60} decomposition on Si(100) Surfaces. Applied Surface Science, 2001, 184, 50.

(32) Pesci, A.; Cepek, C.; Sancrotti, M.; Ferrari, L.; Capozi, M.; Perfetti, P.; Pedio M. SiC(111) growth by C_{60} decomposition on Si(111) studied by electron spectroscopies. Surf. Sci. 2001, 482-485, 829.

(33) Goldoni, A.; Larciprete, R.; Cepek, C.; Masciovecchio, C.; El Mellouhi, F.; Hudej, R.; Sancrotti M.; Paolucci, G., Tracking Thermally Driven Molecular

Reaction and Fragmentation by Fast Photoemission: C_{60} on Si(111). Surface Review and Letters 2002, 9, 775-781.

(34) Cepek, C.; Schiavuta, P.; Sancrotti, M.; Pedio, M., Photoemission study of C_{60}/Si(111) adsorption as a function of coverage and annealing temperature. Phys Rev B 1999, 60, 2068.

(35) Cheng, C. P.; Huang, J. W.; Pi, T. W.; Lee H.-H., Surface structure of SiC formed by C_{60} molecules on a Si(001)-2x1 surface at 800 degrees., J. Appl. Phys. 2006, 99, 123708-1 123708-5.

(36) Pedio , M.; Borgatti, F.; Giglia, A.; Mahne, N.; Nannarone, S.; Giovannini, S.; Cepek, C.; Magnano, E.; Bertoni, G.; Spiller, E.; Sancrotti, M.; Giovanelli, L.; Floreano, L.; Gotter, R.; Morgante A., Annealing Temperature Dependence of C_{60} on Silicon Surfaces: Bond Evolution and Fragmentation as Detected by NEXAFS. Physica Scripta. 2005, T115, 695–698,

(37) Yan-Fang, L.; Jin-Feng, L.; Peng-Shou X.; Hai-Bin P. X-Ray Photoelectron Spectroscopy and Reflection High Energy Electron Diffraction of Epitaxial Growth SiC on Si(100) Using C_{60} and Si. Chinese Physics Letters 2007, 24, 2022-2024.

(38) Wilk, G. D.; Wei, Y.; Edwards, H.; Wallace, R. M. In situ Si flux cleaning technique for producing atomically flat Si(100) surfaces at low temperature. Appl. Phys. Lett., 1997, 70, 2288-2290.

(39) Portail, M.; Zielinski, M.; Chassagne, T.; Roy, S.; Nemoz, M. Comparative study of the role of the nucleation stage on the final crystalline quality of (111) and (100)

silicon carbide films deposited on silicon substrates. Journal of Applied Physics 2009, 105 , 083505 (1-7).

(40) Severino, A.; D'Arrigo, G.; Bongiorno, C.; Scalese, S.; La Via, F.; Foti, G. Thin crystalline 3C-SiC layer growth through carbonization of differently oriented Si substrates. J. Appl. Phys. 2007, 102, 023518 (1-10).

(41) Severino A.; Frewin, C.; Bongiorno, C.; Anzalone, R.; Saddow, S. E.; La Via, F. Structural defects in (100) 3C-SiC heteroepitaxy: Influence of the buffer layer morphology on generation and propagation of stacking faults and microtwins. Diamond & Related Materials 2009, 18, 1440–1449.

(42) Zhao, Z.; Li, Y.; Yin, Z.; Li, Z. Effect of C/Si ratio on the characteristics of 3C-SiC films deposited on Si(100) base on the four-step non-cooling process. Superlattices and Microstructures 2016, 99, 131-135

(43) Kern, W. Handbook of Semiconductor Wafer Cleaning Technology, Noyes Park Ridge, N.J. (1993)

(44) Gray, S. M.; Johansson, M. K.-J.; Johansson, L. S.O. Nanoscale roughening of Si(001) by oxide desorption in ultrahigh vacuum. J. Vac. Sci. Tech B 1996, 140, 1043.

(45) Krause, S.; Schöll, A.; Umbach, E. Determination of transport levels of inorganic semiconductors by ultraviolet and inverse photoemission. Phys. Rev. B 2015, 91, 195101.

(46) Ferrer, S.; Comin F. Rev. Sci. Instrum. 1995, 66, 1674; Balmes, O.; van Rijn, R.; Wermeille, D.; Resta, A.; Petit, L.; Isern, H.; Dufrane, T.; Felici, R. The ID03

surface diffraction beamline for in-situ and real-time X-ray investigations of catalytic reactions at surfaces. Catal. Today 2009, 145 , 220−226.

(47) Yang, Y-N; Williams, E. D. The role of carbon in the faceting of Silicon surfaces on the (111) to (001) azimuth. J. Vac. Sci. Technol. 1990, A8, 2481-2488.

(48) Soukiassian, P. G.; Enriquez, H. B. Atomic scale control and understanding of cubic silicon carbide surface reconstructions, nanostructures and nanochemistry. J. Phys. Condens. Matter 2004, 16, S1611.

(49) Bermudez, V. M.; Long J. P. Characterizaton of reconstructed SiC(100) surfaces using soft-x-ray photoemission spectroscopy. Appl. Phys. Lett. 1995, 66, 475-477.

(50) Santoni, A; Lancok, J.; Dhanak, V.R.; Loreti, S.; Miller, G.; Minarini, C. A. valence-band and core-level photoemission study of a-Si_xC_{1-x} thin films grown by low-temperature low-pressure chemical vapour deposition. Appl. Phys. 2005, A 81, 991–996 .

(51) Kuzubov, A. A.; Eliseeva, N. S.; Krasnov, P. O.; Tomilin, F. N.; Fedorov, A. S.; Tolstaya, A. V. Theoretical study of the thermodynamic stability and electronic structure of thin films of 3C, 2H, and 2D silicon carbidesPhys. Solid State 2014, 56, 1654-1658.

(52) Benesch, C.; Merz, H.; Zacharias, H. Unoccupied surface states of the 3x2-reconstructed 3C-SiC(001) surface. Phys. Rev. B 2002, 65, 235317.

(53) Ostendorf, R.; Benesch, C.; Hagedorn, M.; Merz, H.; Zacharias, H. Unoccupied surface states of the c(2x2)-reconstructed 3C-SiC(001) surface. Phys. Rev. B 2002, 66, 245401.

(54) Note: The rigid shift of our spectra with respect to the literature results is related to the different doping of the Silicon substrate.

(55) Hens, P.; Brow, R.; Robinson, H.; Cromar, M.; Van Zeghbroeck, B. Epitaxial growth of cubic silicon carbide on silicon using hot filament chemical vapor deposition. Thin Solid Films, 2017, 635, 48–52.

(56) David Nečas and Petr Klapetek, Czech Metrology Institute, 2020, Gwyddion-Free SPM data analysis software 2.61 (http://gwyddion.net)

(57) Roh, J. I.; Lee, K. S.; Lee S. H.; Nahm, K. S.; Kim, K. C.; Lim K. Y. Homo-Epitaxial Growth of 3C-SiC(100) Thin Films on SiC/Si Substrate Treated by Chemical Mechanical Polishing. Journal of the Korean Physical Society 2003, 43, 96-101.

(58) Van Hove, J. M.; Pukite, P.; Cohen, P. I. RHEED streaks and instrument response. J. Vac. Sci. Technol. A 1983, 1 ,609.

(59) Björck M.; Andersson, G. *GenX*: an extensible X-ray reflectivity refinement program utilizing differential evolution. J. Appl. Cryst. 2007, 40, 1174-1178.

(60) Presser, V.; Nickel, K. G. Silica on Silicon Carbide" Critical Reviews in Solid State and Materials Sciences, 2008, 33, 1–99.

For Table of Contents Use Only

Tuning 3C-SiC(100)/Si(100) Heterostructure Interface Quality

Maddalena Pedio, Elena Magnano, Paolo Moras, Francesco Borgatti, Roberto Felici, Barbara Troian, Stefano Prato, Cristian Soncini, and Cinzia Cepek